RRB 88-101

UTILIZING VEGETATION VIGOR AS AN AID TO ASSESSING GROUNDWATER FLOW PATHWAYS FROM SPACE

by

R.P. Bukata, J.E. Bruton and J.H. Jerome

Rivers Research Branch
National Water Research Institute
Canada Centre for Inland Waters
Burlington, Ontario, L7R 4A6

December 1988
NWRI Contribution #89-59

ABSTRACT

There currently exists a large volume of satellite data spanning the passive visible and near-infrared radiance responses. This work investigates the ability of such optical data to delineate groundwater flow pathways in a freshwater basin by utilizing the vigor of the vegetative cover to delineate the discharge, recharge and transition areas defining that basin. Selecting the Big Otter and Big Creek basins in southern Ontario, Canada (both of which drain into northern Lake Erie), such analyses were shown to be very effective in delineating groundwater flow regimes for the LANDSAT-1 overpass of July 6, 1974 when the basin was under maximum state of vegetation bloom. The seasonal growth cycles of the indigenous natural and cultivated crop canopies and their impact on such classification activities are also discussed.

RÉSUMÉ

Nous disposons actuellement d'un grand nombre de données satellite qui couvrent les réponses passives de radiance dans les domaines du visible et du proche infrarouge. Cette étude a pour but de vérifier si ces données optiques peuvent être utiles pour déterminer les voies d'écoulement des eaux souterraines d'un bassin hydrographique d'eau douce à l'aide des données relatives à la vigueur du couvert végétal, indice utilisé pour délimiter les zones d'émergence, d'alimentation et de transition qui définissent ce bassin. Nos analyses, portant sur les bassins de Big Otter et de Big Creek dans le sud de l'Ontario au Canada (ces deux bassins se jettent dans le nord du lac Érié), se sont avérées très efficaces pour déterminer les régimes d'écoulement des eaux souterraines au moment du passage du satellite LANDSAT-1 au-dessus de cette région le 6 juillet 1974, date à laquelle ce bassin était au plus fort de sa période de végétation. Les cycles de croissance saisonniers des plantes naturelles indigènes et des plantes cultivées de même que l'impact de ces cycles sur ce type d'analyses sont aussi examinés.

MANAGEMENT PERSPECTIVE

This manuscript was specifically requested by the Soviet Academy of Sciences during an invited presentation by the senior author at the Headquarters of the Leningrad Chapter of the Soviet Academy. It was the Academy's stated hope that this unique Canadian experience if applied to groundwater flow pathways around Soviet nuclear power installations would assist in preventing civil disasters such as the Chernobyl incident.

PERSPECTIVE-GESTION

Cette étude a été spécifiquement demandée par l'Académie des sciences de l'URSS à l'occasion d'un exposé présenté par l'auteur principal de cette étude. Ce dernier était alors invité au Bureau central de la Section de Leningrad de l'Académie soviétique. Cette réalisation canadienne originale a suscité à l'Académie l'espoir que cette méthode, appliquée aux voies d'écoulement des eaux souterraines circulant autour des centrales nucléaires soviétiques, aide à prévenir certains désastres civils comme l'incident de Tchernobyl.

INTRODUCTION

The rigorous scientific description of groundwater hydraulic flow logically incorporates the interactive natures of the governing meteorological conditions, basin morphology, soil dynamics, and biochemical properties of the indigenous vegetative canopies. Such interactions must further be considered within a realistic appraisal of the temporal and spatial variabilities defining this complement of controlling parameters. Nonetheless, a valuable input to the assessment of groundwater flow within a basin or watershed is the identification of the groundwater regimes comprising that basin or watershed. Once a reliable delineation of the principal groundwater regimes is established, a synoptic representation of the principal directions of groundwater flow, on a variety of spatial scales, may be readily obtained for the basin under study.

There will soon exist two decades of available environmental satellite data. Such a terrestrial optical data base presents the opportunity for not only delineating such groundwater regimes, but also providing historical insights into their temporal and spatial evolutions. Since the vast majority of this available data are comprised of passive visible and near-infrared radiance, the possibility of utilizing such radiance responses in delineating hydraulic flow should be investigated.

This work discusses the application of telemetered LANDSAT data to the synoptic classification of a freshwater basin within the

Laurentian Great Lakes system in southern Ontario, Canada, in terms of its component groundwater regimes. These groundwater regimes are considered to be:

a) Discharge Areas - those regions of the basin in which the water table is in close proximity to the terrain surface. The ultimate discharge area is, therefore, defined by open water.

b) Recharge Areas - those regions of the basin in which the water table is substantially below the terrain surface.

c) Transition Areas - those regions of the basin which, due to the intermediate depth of the water table, represent aquatic regimes distinct from both the discharge and recharge areas. However, under conditions of excessive precipitation or drought, such areas may assume the characteristics of discharge or recharge areas, respectively. The transition areas of a basin or watershed generally represent the most desirable land from an agricultural standpoint. They also, however, represent the agricultural land most vulnerable to flooding.

The freshwater basins comprising the Canadian Great lakes region sustain seasonal cycles of vegetation cover. This vegetation cover, whether natural or deliberately cultivated, contains predominantly

phreatophytic (water-loving) species which rely upon non-saline water supplies for life, growth and vigor. Chlorophyll concentrations within the plant cells are generally considered representative measures of the stage of plant development and vigor. Since chlorophyll has long been observed to strongly absorb impinging visible radiation and strongly reflect impinging near-infrared radiation, healthy vegetation (i.e., high degree of vigor) as viewed from satellite sensors during summer months (or peaks of growth seasons) should be characterized by low visible radiance values and high near-infrared radiance values. Further, since the vigor of such vegetative cover would be inversely proportional to the depth of the water table, it is reasonable to suggest that natural vegetation associated with discharge areas would be observed from space as being comprised of pixels (picture-scene elements) which displayed high near-infrared radiance values coupled with low visible radiance values. Similarly, the less vigorous natural vegetation associated with recharge areas would be observed from space as being comprised of pixels which displayed lower near-infrared radiance values coupled with higher visible radiance values than those pixels defining discharge areas.

Figure 1 illustrates a hypothetical "clustering" of pairs of radiance responses (near-infrared and visible) which might logically result from a correlation involving the totality of pixels obtained from a satellite overview of a freshwater basin under full vegetative canopy. A "vigor curve" might readily emerge, along which the location of the pixel radiance pairs would be indicative of the degree of

vigor (chlorophyll/water relationship) characterizing the indigenous foliage. The three illustrated clustering distributions labelled "Discharge Areas", "Recharge Areas" and "Transition Areas" in Figure 1 would therefore refer to basin regions defined by relatively lush vegetation (i.e., water table close to the surface), relatively sparse vegetation (i.e., water table substantially removed from the surface), and vegetation of intermediate vigor, respectively.

The exact shape and size of the three anticipated distributions along the "vigor curve" would be totally dependent upon the percentages of each of the three principal groundwater regimes present within the basin at the time of satellite overpass, and will vary dramatically from basin to basin (e.g., wetland wildlife habitats would be heavily weighted towards the discharge area distribution, while poorly-irrigated basins would be heavily weighted towards the recharge area distribution). Further, the "vigor curve" for the same basin will display ephemeral variations directly controlled by the fluctuations of the governing climatic factors and the biological life-cycles of the indigenous verdure.

Such visible/near-infrared clustering techniques have been in widespread use for monitoring agricultural biomass since the "tasseled-cap" transformations of the four LANDSAT bands first proposed by Kauth and Thomas (1976). These orthogonal linear transformations yielded sets of brightness, greenness, yellowness, and nonesuch classification indices which were extended by Richardson and Wiegand (1977), Dave (1981), Jackson (1983), Gallo and Daughtry

(1987), and others to include sets of vegetation indices which could be utilized for such computer classification activities as soil distinctions, crop identification, and biomass estimations. Such vegetation and/or soils cataloging is not the intention of the present regional scale mapping exercise. Rather, the intention here is to relate, in as simple an operational procedure as feasible, vigor of ground cover in a freshwater basin to the principal groundwater flow regimes controlling the drainage patterns of that basin. Consequently, the mid-summer (anticipated time of maximum chlorophyll bloom) clustering of visible/near-infrared radiances along an anticipated "vigor curve" such as depicted in Figure 1 will be investigated as a possible means of obtaining such a simple operational procedure.

TEST SITE

Figure 2 shows the physical location of the Big Creek and Big Otter Creek basins in southern Ontario, Canada. These freshwater basins are included within the Great Lakes system, and both basins drain into northeastern Lake Erie. The bedrock of the basin consists predominantly of limestone, dolomite, and shale with the general slope of the bedrock surface directed southward, and the major surficial deposits comprising the basins being sand and till. The surficial geology (Sibul, 1969; Yakutchik and Lammers, 1970) of the test basins is schematically illustrated in Figure 3. These basins play a vital role in the economy of southern Ontario, a direct consequence of the

extensive farming activities utilizing the basin terrain during the summer season.

LANDSAT-1 digital data were obtained for the virtually cloud-free July 6, 1974 satellite overpass depicting the basins under mid-summer conditions. The basins were defined by ~350,000 pixels of ground resolution ~80 m x 60 m. Data from the visible red wavelength band (0.6 to 0.7 μm) and the near-infrared wavelength band (0.8 to 1.1 μm) were intercorrelated in the manner conceptualized in Figure 1. (The intermediate LANDSAT band of wavelength interval (0.7 to 0.8 μm) must be carefully avoided in this type of clustering activity since this wavelength interval straddles both the visible and near-infrared regions of the electromagnetic spectrum and is therefore unsuitable, at least in this instance, for recording the optical signatures of chlorophyll concentrations.)

Figure 4 illustrates the red/near-infrared correlation resulting from the 27,864 pixels comprising the selected training area (near Scotland, Ontario) on July 6, 1974. Also shown in Figure 4 are the visible red and near-infrared pixel distribution histograms. Evident in the figure are the three anticipated distributions lying along a principal curve defining the vigor of the vegetative canopy.

A cone of transition zone pixels may be estimated from Figure 4, and the pixels included within this cone should contain most of the prime agricultural land indigenous to the basins. It is also evident that, although the data do lie roughly along the curve defining the vigor of natural vegetation, there is the not-unexpected statistical

scatter and lateral spread resulting from human intervention within the basins (farm buildings, road networks, tobacco drying sheds, etc.). Discharge areas are particularly well-aligned with the "vigor curve" since the vegetation encountered in most of these areas is unaffected by the commercial activities occurring within the basin. However, it is seen that extended statistical spread occurs in the vicinities of the recharge areas with the pixel distribution showing considerable departure from the natural vigor curve and displaying a very obvious invasion into the distribution defining the transition zone areas. This is almost completely due to the fact that the basin is largely worked as farmland, and many of the farms are located on the recharge plains, the least desirable land from an agricultural standpoint. Modern agricultural practices (judicious choice of crops, irrigation schemes, soil conditioning, for example) act in such a manner as to improve the vigor and yield of the land, and thus result in a movement of the pixel radiance values along the natural vigor curve towards regions of more lush vegetation. The degree of invasion of the recharge area distribution into the cone of transition in two-band scatter correlations such as shown in Figure 4, therefore, reflects the degree of success resulting from such attempts to increase the cultivated crop yields of the basin.

GROUNDWATER REGIME CLASSIFICATIONS

Computer programs were written to display a) those pixels from Figure 4 which were clustered to the left of the upper line defining

the cone of transition, b) those pixels which were clustered to the right of the lower line defining the cone of transition, and c) those pixels which were clustered between the two lines defining the cone of transition.

Figure 5 illustrates a computer printout of the pixels to the left of the cone of transition, and which are taken to represent the discharge areas in the Scotland training centre. Figure 6 illustrates a computer printout of the pixels to the right of the cone of transition, and which are taken to represent the recharge areas in the Scotland training centre.

Remote thermal sensors have been in widespread use for several decades, and have been successfully applied by many workers to such areas as thermal effluent plumes, groundwater discharges into lakes and streams, lake surface temperature mapping, the location of artesian wells, toxic waste impact assessments, and related basin features (see, for example, Moore et al., 1972; Boettcher et al., 1976; Brown, 1972; Rundquist et al., 1985; Tracey and Lawrence, 1983; Pluhowski, 1972; Philpot and Philipson, 1985; amongst numerous others). And although such studies have predominantly concentrated upon relatively localized environmental targets such as river mouths, wells, aquifers, estuaries, etc., and surprisingly little work has been directed towards basinwide regional scale classifications of groundwater regimes, it seems not at all unreasonable to consider that, under the optimal set of conditions, a thermal scan of a freshwater basin could yield a thematic map of the principal groundwater

regimes. Such optimal conditions would be the simultaneous occurrence of maximum definition of the thermal gradients being sought and nonoccurrence of obfuscating extraneous thermal intrusions from such sources as sporadic snow, ice, vegetative canopies or anthropogenic activities. Such conditions could reasonably be considered as existing during conditions of late winter or early spring. A thermal scan of the Scotland area during late winter/early spring might therefore be expected to yield a reasonable estimate of the groundwater regimes in such a freshwater basin. The Scotland test area was overflown through the courtesy of the Canada Centre for Remote Sensing on February 12, 1976. Data were collected by a Daedalus infrared scanner (8-14 μm) at an altitude of 4600 feet during pre-dawn hours. A mosaic of imagery so obtained is illustrated in Figure 7. On February 12, 1976, the test area was under almost total snow cover, and since the data were collected during nondaylight hours, Figure 7 may be confidently taken to represent the true thermal regimes comprising the snow-covered basins (see the very brief discussion in the Appendix). Despite the almost two year separation in time between Figure 7 and Figures 5 and 6, the thermal imagery of the Scotland area displayed in Figure 7 is almost identical to the computer classifications of Figures 5 and 6 (allowing for the lack of geographic pixel registration characterizing the computer printouts). Particularly excellent agreement is seen in the delineations of the two principal discharge areas A and B, the Big Creek tributary, and the smaller discharge area between the major discharge areas. The only significant difference

between the two sets of data is the presence of a surficial aquifer which was evident during the 1976 airborne scan.

Figure 8 illustrates a computer printout of the pixels contained within the cone of transition. Once the physical locations of discharge, recharge and transition areas are delineated synoptically for a basin or watershed, an assessment of the pathways by which groundwater enters and evacuates from a groundwater regime system may be readily determined.

Figure 9 combines the Scotland area groundwater regime classifications of Figures 5, 6 and 8 into a single thematic map. The discharge areas are delineated as crosses, the recharge areas as dots, and the transition areas are left as blanks. Following the general rule that groundwater movements within a basin occur from recharge through transition to discharge areas (i.e., from higher to lower elevations in a naturally drained basin, although not necessarily so in an artificially drained basin), a first-order directionality for the groundwater flow pathways in the Scotland area may be as schematically indicated by the flow-line arrows in Figure 9.

The classification determined for the training centre may now be readily extended to include the entire test basin. Figure 10 displays the computer classification for all the discharge areas in the Big Otter and Big Creek basins as delineated by the LANDSAT-1 earth-orbiting satellite on July 6, 1974. Clearly delineated are the Big Creek and Big Otter Creek main drainage patterns responsible for the evacuation of groundwater discharge from these basins into northeastern Lake Erie. The computer classification of satellite data

depicted in Figure 10 may be directly compared to the distribution of groundwater discharge areas (after Novakovic and Farvolden, 1974) shown in Figure 11. This thematic map was constructed solely from drilled well and other ground-acquired data collected in the basins during about a two and a half year period. Clearly, the digital data acquired by the LANDSAT-1 space vehicle in less than 20 seconds successfully delineated all the major tributaries covered by the Novakovic and Farvolden studies. In addition, further dendritic patterns emerge from the satellite data which would be either excessively time-consuming or physically inaccessible for ground-based investigative teams to explore fully. This is particularly evident in the area north of Lake Erie between Port Burwell and Long Point, a wetland region not included in the earthbound studies, but most important to the overall groundwater input to Lake Erie.

IMPACT OF SEASONAL GROWTH CYCLES ON GROUNDWATER REGIME CLASSIFICATIONS

The vigor curve of Figure 1 will, of course, display a seasonal variation which follows the growth cycle of the phreatophytic natural and cultivated canopies pertinent to the basins under study. Such a temporal evolution of near-infrared versus visible red radiance correlations are shown in Figure 12. Most of the radiance data depicted therein are for available 1973 overpasses of the Scotland training area by LANDSAT-1, although the July 6, 1974 overpass (Figure 4) is also included. Clearly, the correlations are seen to

logically progress from a linear correlation (with discharge areas clustered at lowest values of radiance for both visible and near-infrared spectral regions) during the winter months, through a quasi-clockwise rotation in the spring as the chlorophyll growth matures to the mid-summer vigor curve of Figure 1 (with the discharge areas clustered at low values of visible radiance coupled with high values of near-infrared radiance). Subsequent to the mid-summer peak of chlorophyll concentration, the correlation will return to the winter linear correlation through a quasi-counterclockwise rotation during the autumn months. The southern Ontario basins considered in this study are comprised primarily of water loving vegetative canopies that shed their leaves during the winter season, with the coniferous stand being of relative insignificance. The bulk of the evergreen stand present in the basin comprises cultivated windbreaks which occupy areal extents small in comparison to the resolution elements of the satellite sensors. For a basin in which the coniferous stand comprises a significant percentage of the vegetative cover, the seasonal visible/near-infrared correlations, would of course, be defined by a curve which would reflect the year-round presence of chlorophyll concentrations. For example, the spring correlations might display a cross-like correlation, the result of a superposition of a linear correlation (such as the February and March correlations of Figure 12) representing the radiance response of that portion of the basin characterized by deciduous foliage and a "vigor curve"

correlation (such as the mid-summer correlations of Figure 12) representing the radiance response of that portion of the basin characterized by coniferous foliage.

APPENDIX

THERMAL GRADIENTS AS A MEANS OF ASSESSING GROUNDWATER FLOW

Figure 13 conceptualizes the physical principles of groundwater flow in a recharge/discharge basin subsystem during the winter and summer seasons. During winter, water entering a recharge area is colder than the water ultimately arriving at a discharge area. Conversely, during summer, water entering a recharge area is warmer than the water ultimately arriving at a discharge area.

Assuming the not unreasonable working hypotheses that:

(i) measurable thermal gradients exist in the groundwater flow system between recharge and discharge areas

(ii) surficial thermal gradients may be considered to be manifestations of subsurface thermal gradients

(iii) the intensity of these surficial manifestations of subsurface thermal gradients is inversely proportional to the depth of the water table,

then a synoptic overview which is capable of responding to a distinct pattern of lateral (and, if possible, vertical) thermal gradients may play an important role in classifying the principal groundwater regimes in a freshwater basin.

REFERENCES

Boettcher, A.J., Haralick, R.M., Paul, C.A., and Smothers, N. (1976). Use of thermal infrared imagery in groundwater investigations, northwestern Montana. J. Res. U.S. Geol. Survey, Vol. 4., No. 6, pp. 727-732.

Brown, M.C. (1972). Karst hydrogeology and infrared imagery: An example. Geol. Soc. Amer. Bulletin. 83, pp. 3151-3154.

Dave, J.V. (1981). Influence of illumination and viewing geometry and atmospheric composition in the "tasseled-cap" transformation of LANDSAT MSS data. Remote Sens. of Environ. 11, pp. 37-55.

Gallo, K.P. and Daughtry, C.S.T. (1987). Differences in vegetation indices for simulated LANDSAT-5 MSS and TM, NOAA-9 AVHRR, and SPOT-1 sensor systems. Remote Sens. of Environ. 23, pp. 439-452.

Jackson, R.D. (1983). Spectral indices in n-space. Remote Sens. of Environ. 13, pp. 409-421.

Kauth, R.J. and Thomas, G.S. (1976). The tasseled cap - A graphic description of the spectral-temporal development of agricultural crops as seen by LANDSAT. Proceedings of the Symposium on Machine Processing of Remotely Sensed Data, Purdue University, West Lafayette, Indiana, pp 41-51.

Moore, D.G., Myers, V.I. and Giles, W.H. (1972). Location of flowing artesian wells using thermal infrared scanning imagery. Interim Technical Report RSI-72-04, Remote Sensing Institute, Brookings, South Dakota, 6 pages.

Novakovic, B. and Farvolden, R.N. (1974). Investigations of groundwater flow systems in Big Creek and Big Otter Creek drainage basis, Ontario. Can. J. Earth Sci., 11, pp. 964-975.

Philpot, W. and Philipson, W. (1985). Thermal sensing for characterizing the contents of waste storage drums. Photogramm. Eng. and Rem. Sens., 51, pp. 237-243.

Pluhowski, E.J. (1972). Hydrologic interpretations based on infrared imagery of Long Island, New York. Geol. Survey Water Supply Paper 1009-B, 20 pages.

Richardson, A.J. and Wiegand, C.L. (1977). Distinguishing vegetation from soil background information. Photogramm. Eng. Remote Sens. 43, pp. 1541-1552.

Rundquist, D., Murray, G., and Queen, L. (1985). Airborne thermal mapping of a "flow-through" lake in the Nebrasaka sandhills. Water Res. Bulletin, Vol. 21, No. 6, pp. 989-994.

Sibul, U. (1969). Water resources of the Big Otter Creek drainage basin. Water Resources Commission Report No. 1, 91 pages.

Tracey, J.P. and Lawrence, G.R. (1983). Classification of groundwater discharge sites using thermal infrared mapping techniques. Proceedings of 8th Canadian Symp. on Rem. Sens., Montreal, Quebec, pp. 755-763.

Yakutchik, T.J. and Lammers, W. (1970). Water resources of the Big Creek drainage basin. Water Resources Commission Report No. 2, 172 pages.

FIGURE CAPTIONS

Figure 1. The anticipated "vigor curve" that might result from correlating the simultaneously recorded visible and near-infrared radiance responses from fully developed phreatophytic natural vegetation.

Figure 2. The location of the Big Creek and Big Otter Creek basins in southern Ontario.

Figure 3. The surficial geology of the test basins.

Figure 4. The near-infrared versus visible red correlation for the Scotland area on July 6, 1974.

Figure 5. Computer printout of the pixels of Figure 4 which are clustered to the left of the upper line defining the cone of transition (taken to represent discharge areas).

Figure 6. Computer printout of the pixels of Figure 4 which are clustered to the right of the lower line defining the cone of transition (taken to represent recharge areas).

Figure 7. Mosaic of the airborne thermal scan of the Scotland area on February 12, 1976.

Figure 8. Computer printout of the pixels of Figure 4 which are clustered within the cone of transition.

Figure 9. First-order determination of groundwater flow pathways in the Scotland area.

Figure 10. Computer classification of discharge areas in the Big Otter and Big Creek basins as determined by LANDSAT-1 on July 6, 1974.

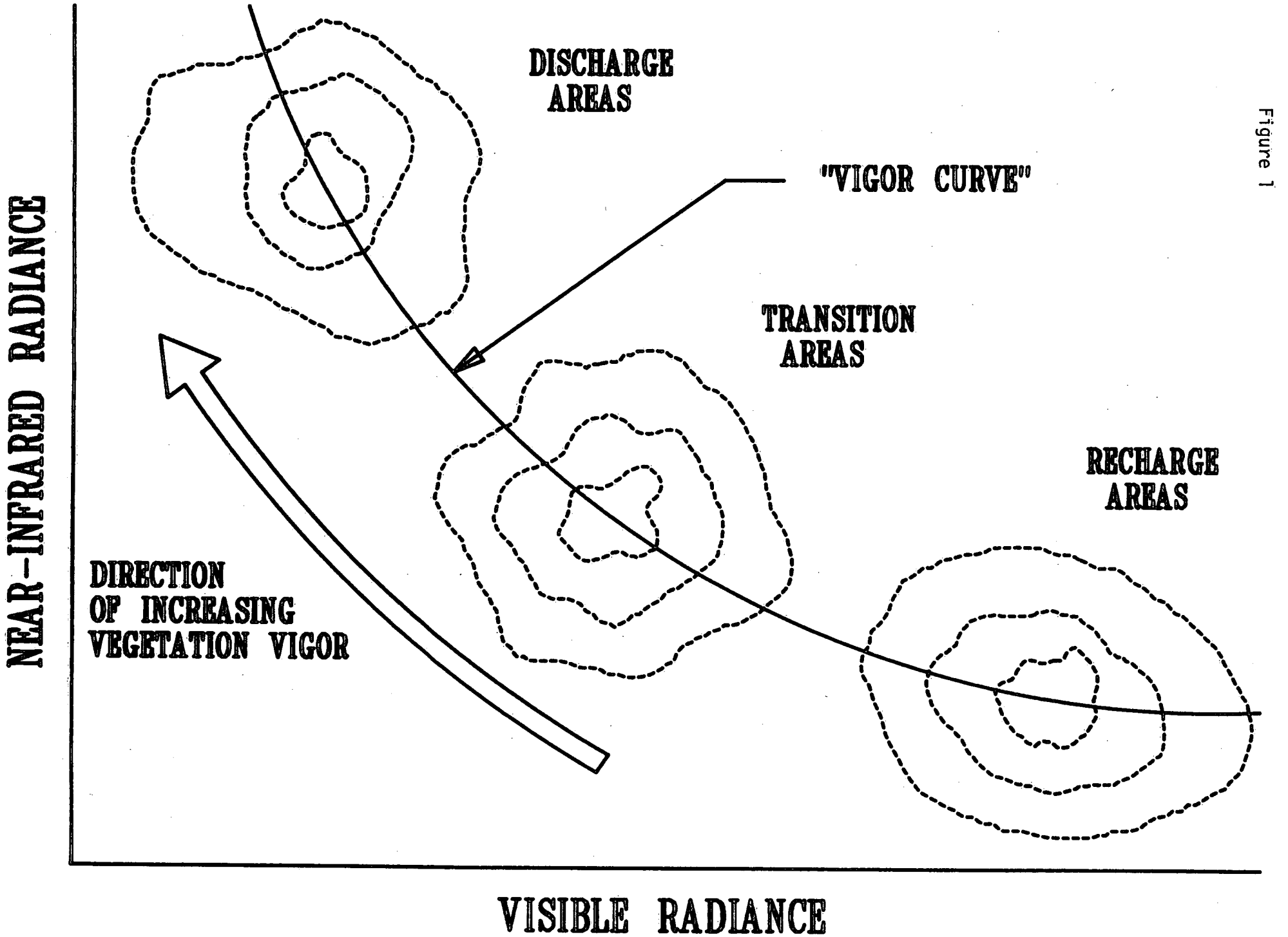
DISCHARGE AREAS
"VIGOR CURVE"
TRANSITION AREAS
RECHARGE AREAS
DIRECTION OF INCREASING VEGETATION VIGOR
NEAR-INFRARED RADIANCE
VISIBLE RADIANCE

Figure 1

Figure 2

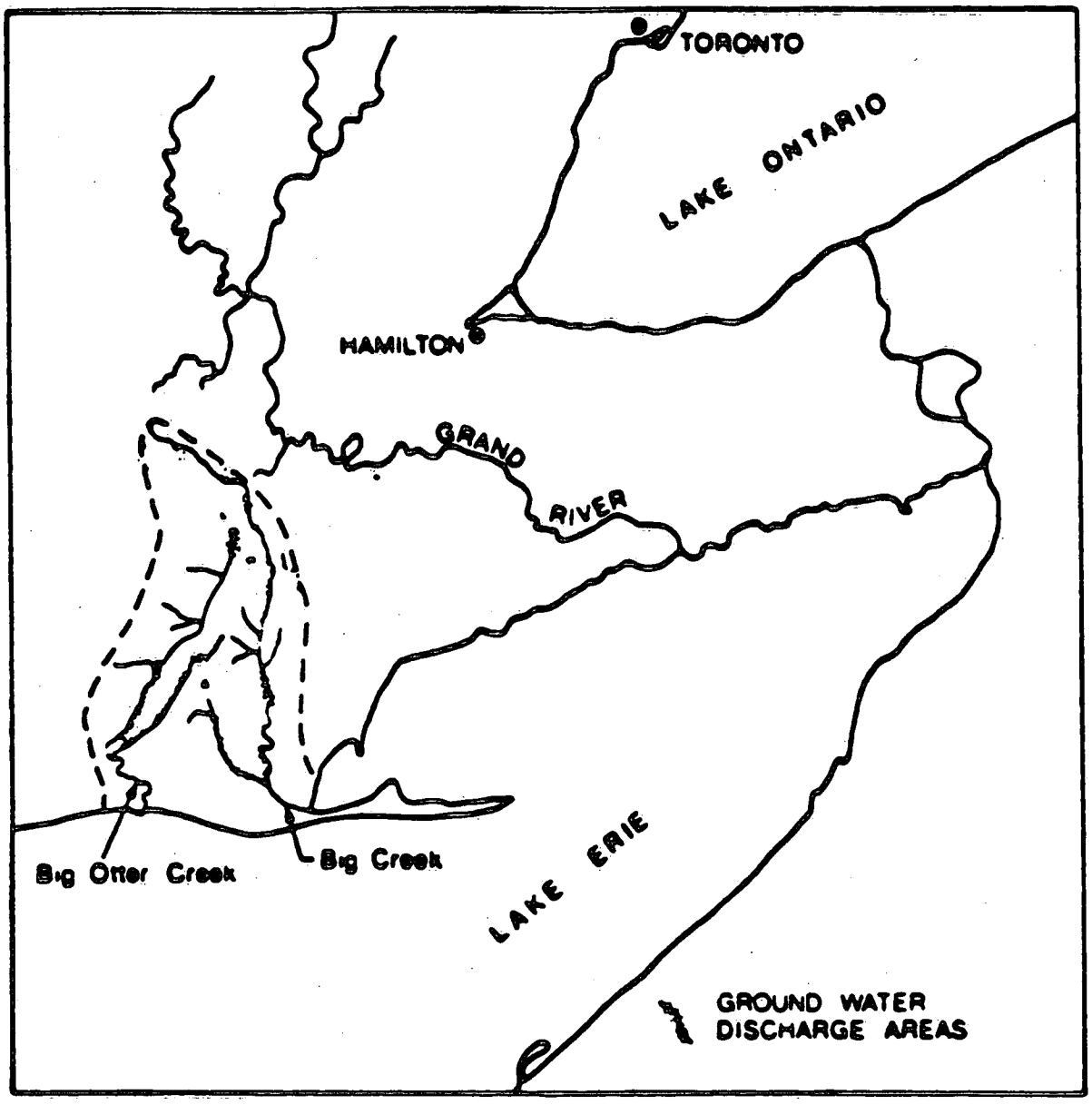

FIGURE 2

Figure 3

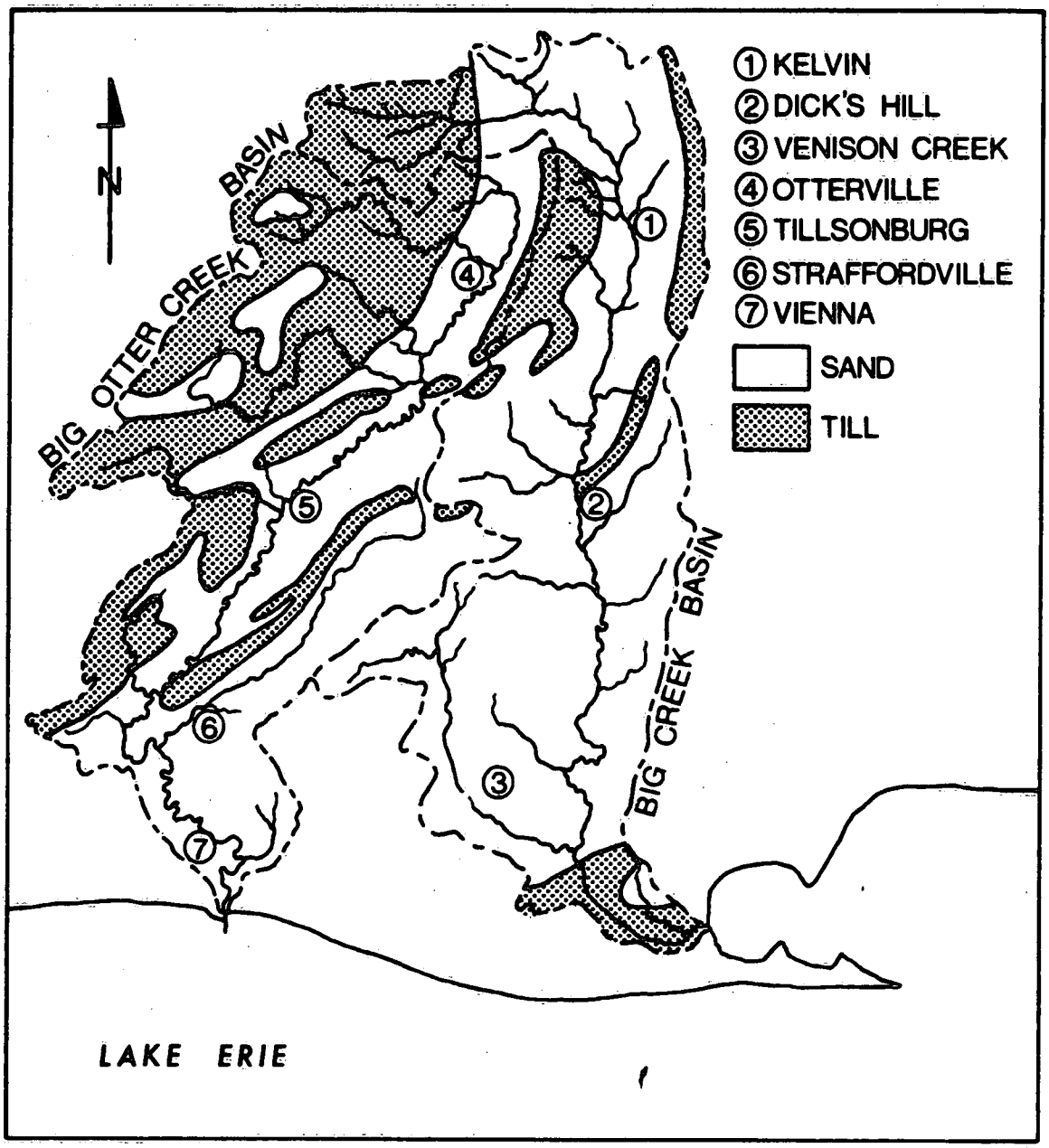

SURFICIAL GEOLOGY (After SIBUL 1969; YAKUTCHIK and LAMMERS 1970.)

Figure 4

TRAINING CENTRE
(SCOTLAND AREA)

Landsat-1 Data for Overpass on July 6, 1974

(27,864 PIXELS)

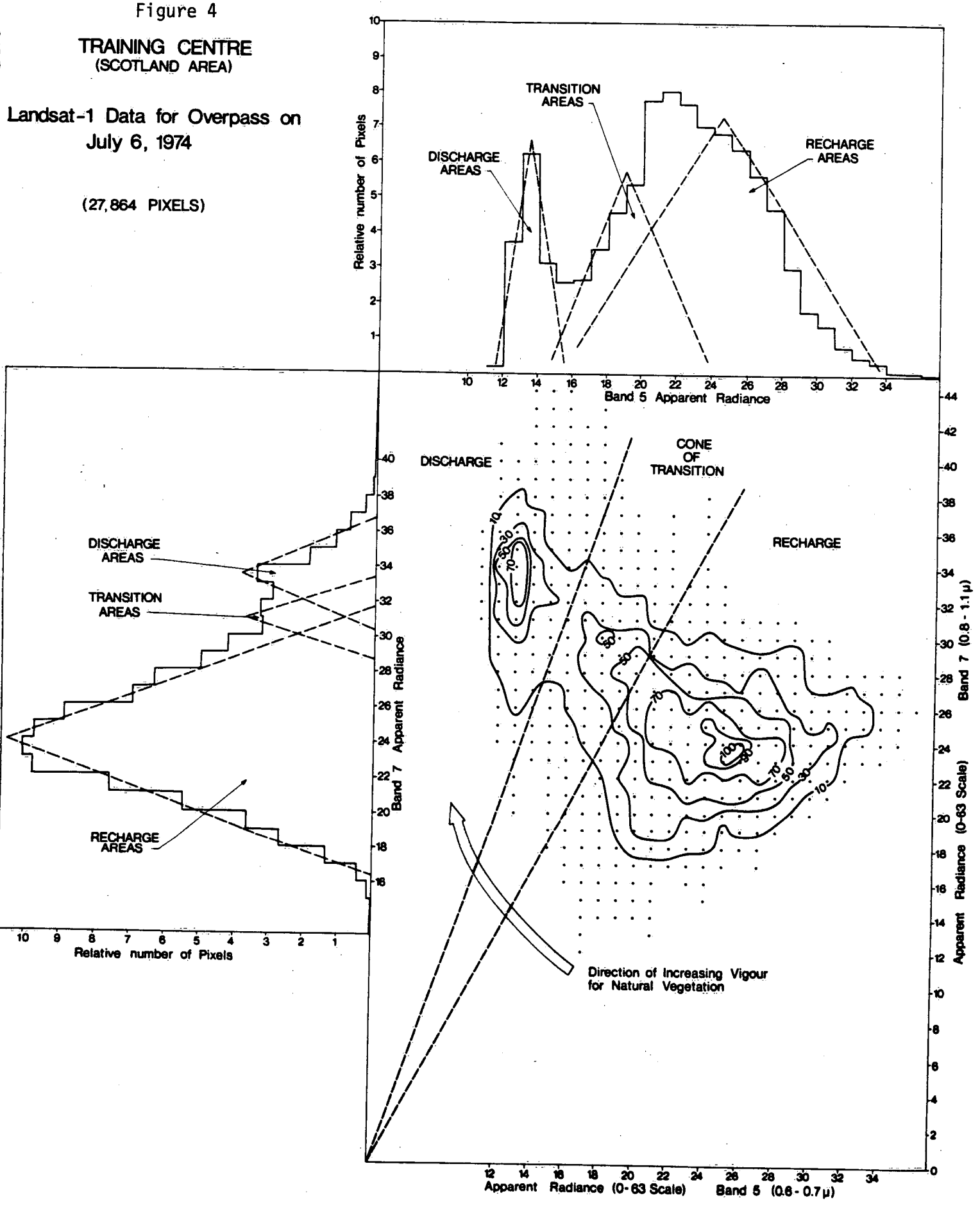

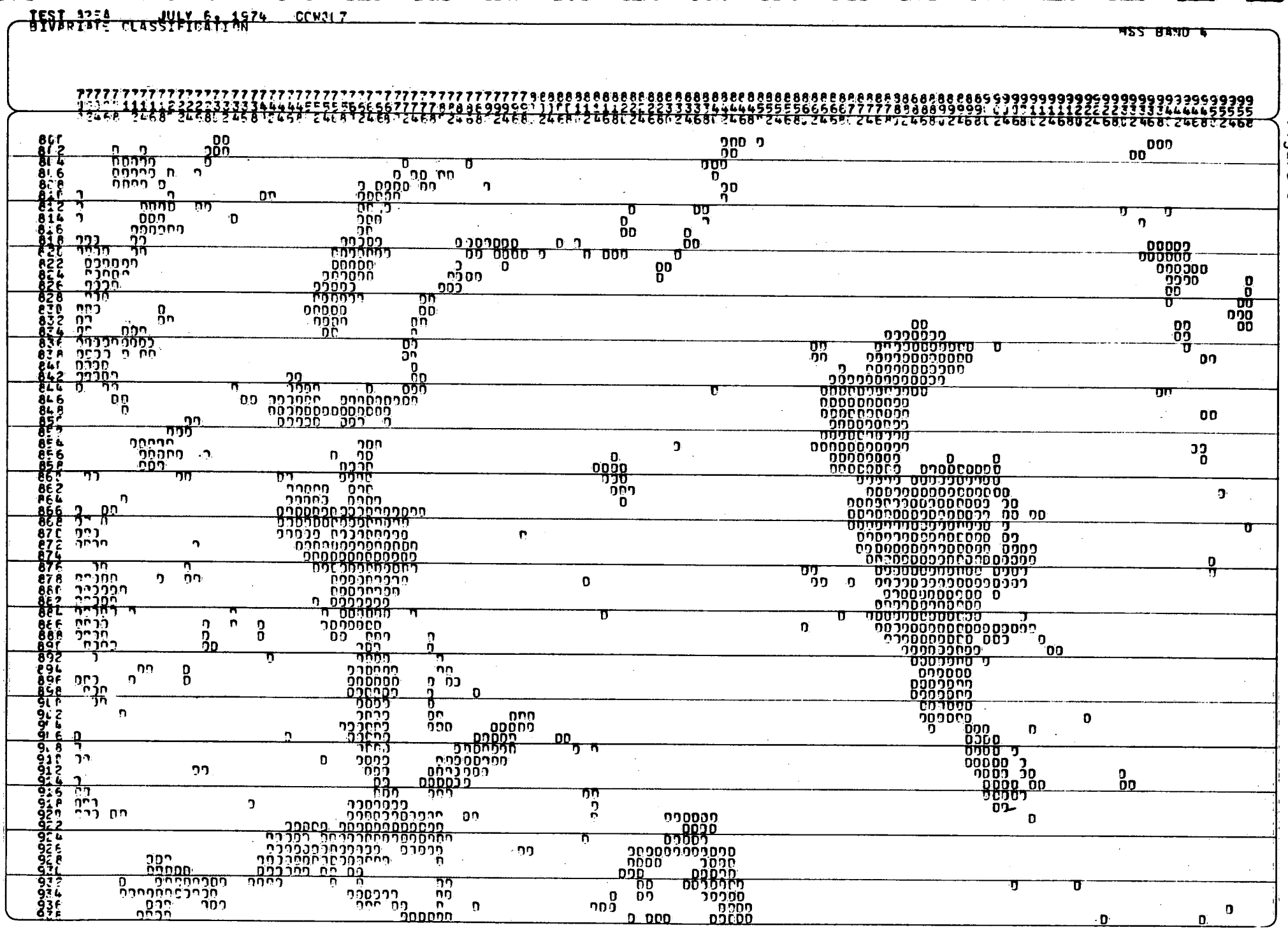
TEST 3258 JULY 6, 1974 CCW317
BIVARIATE CLASSIFICATION
MSS BAND 4

Figure 5

TEST AREA JULY 6, 1974 CCW..7

BIVARIATE CLASSIFICATION

MSS BAND 4

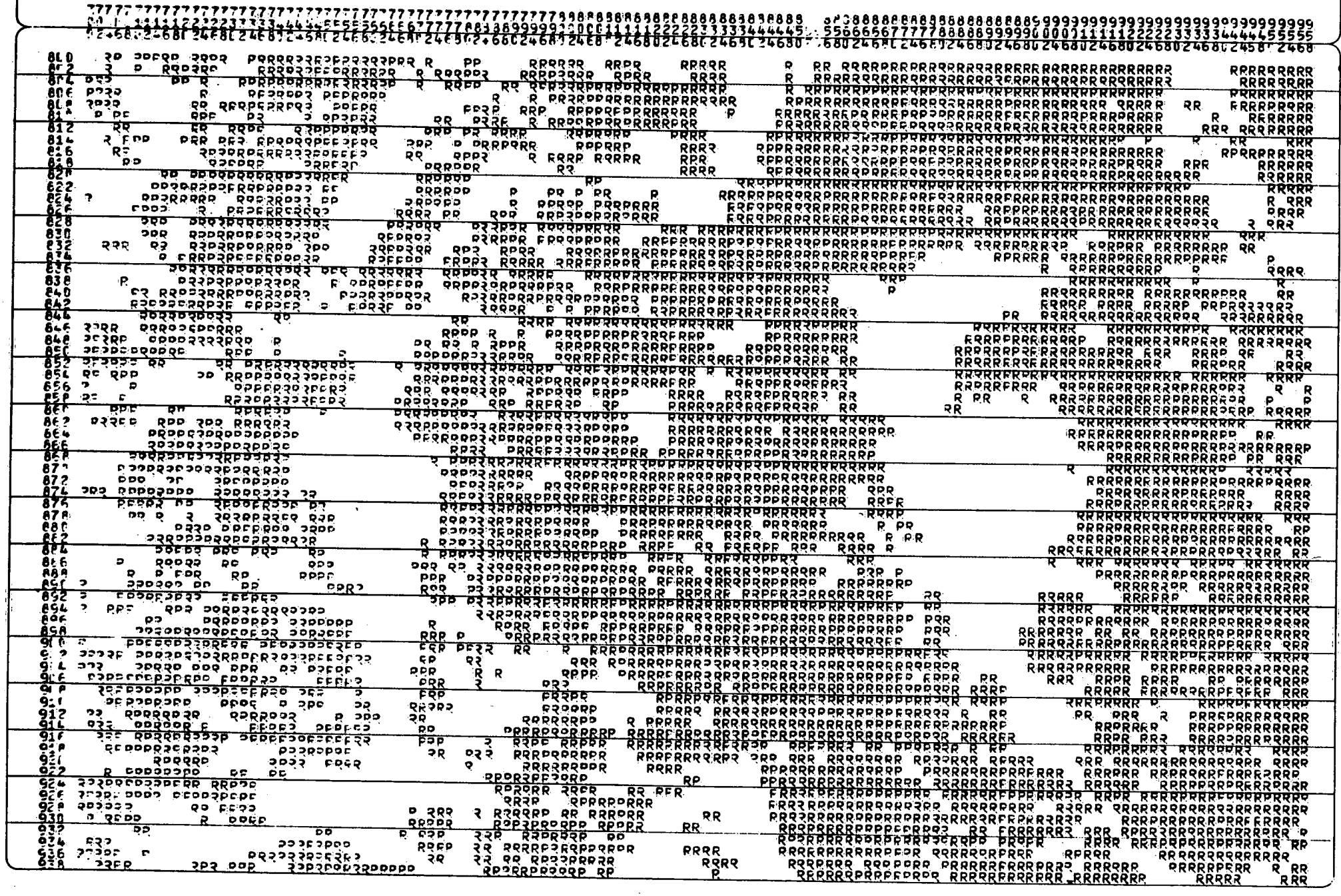

Figure 6

Figure 7

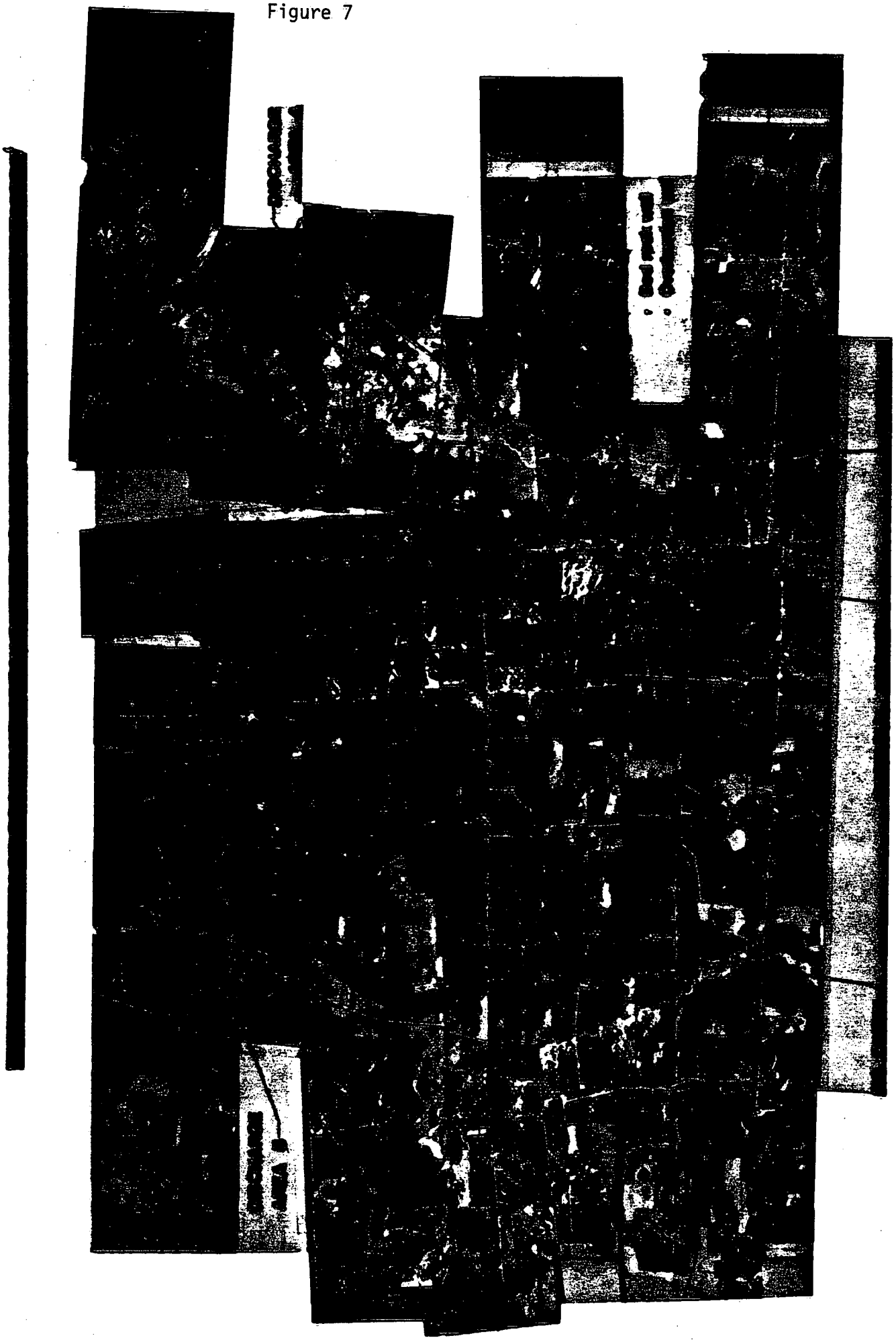

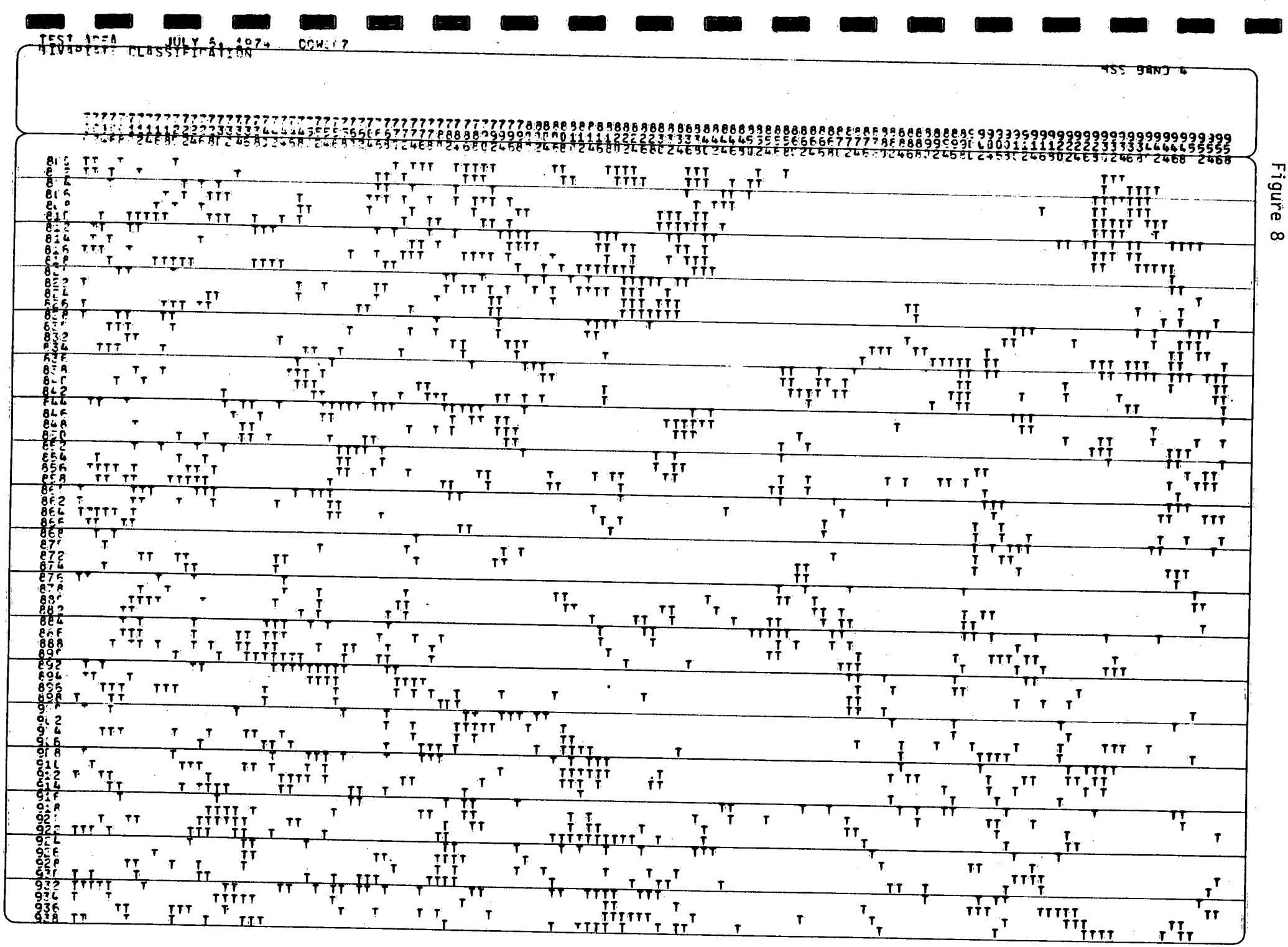

Figure 8

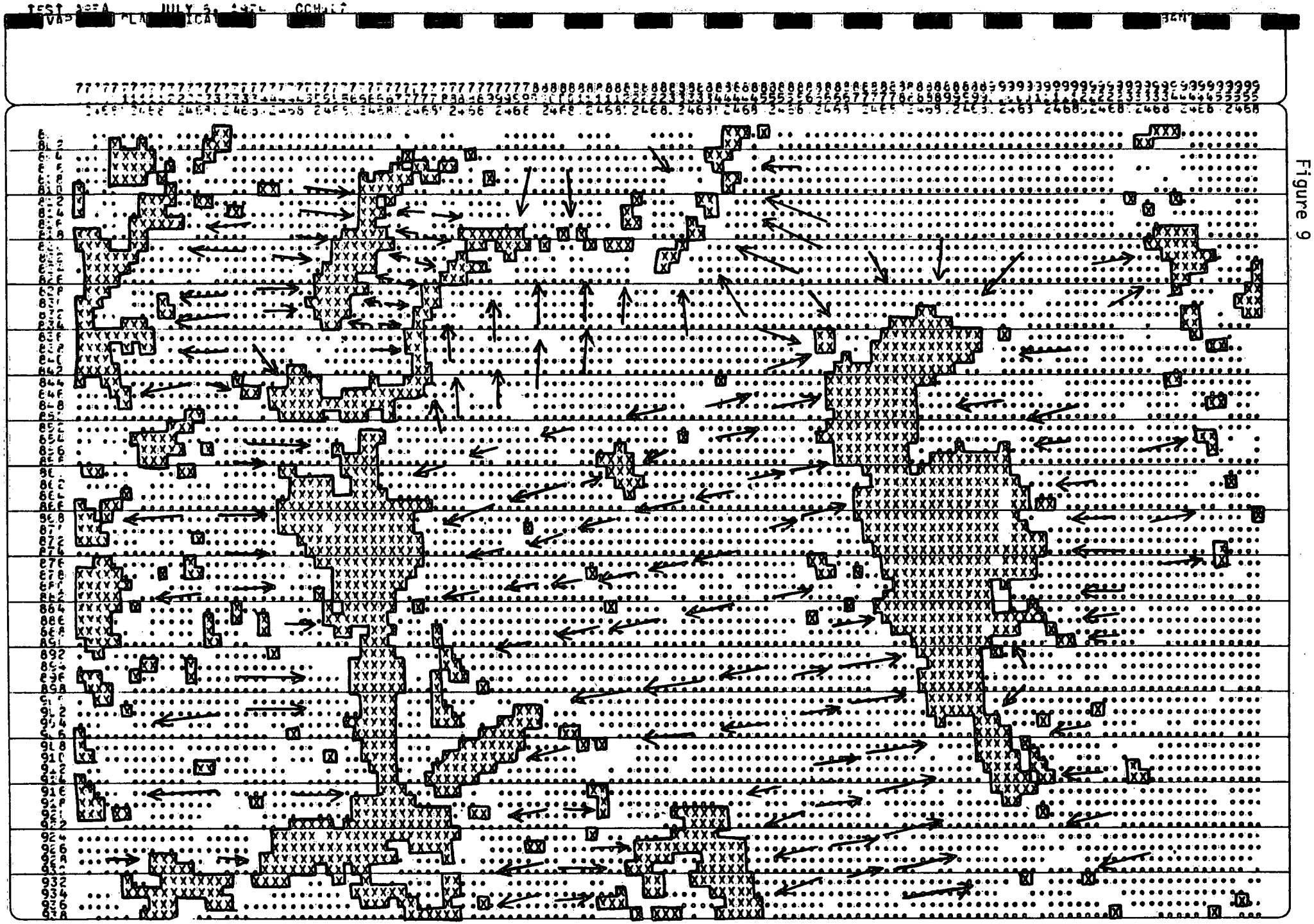

Figure 9

Figure 10

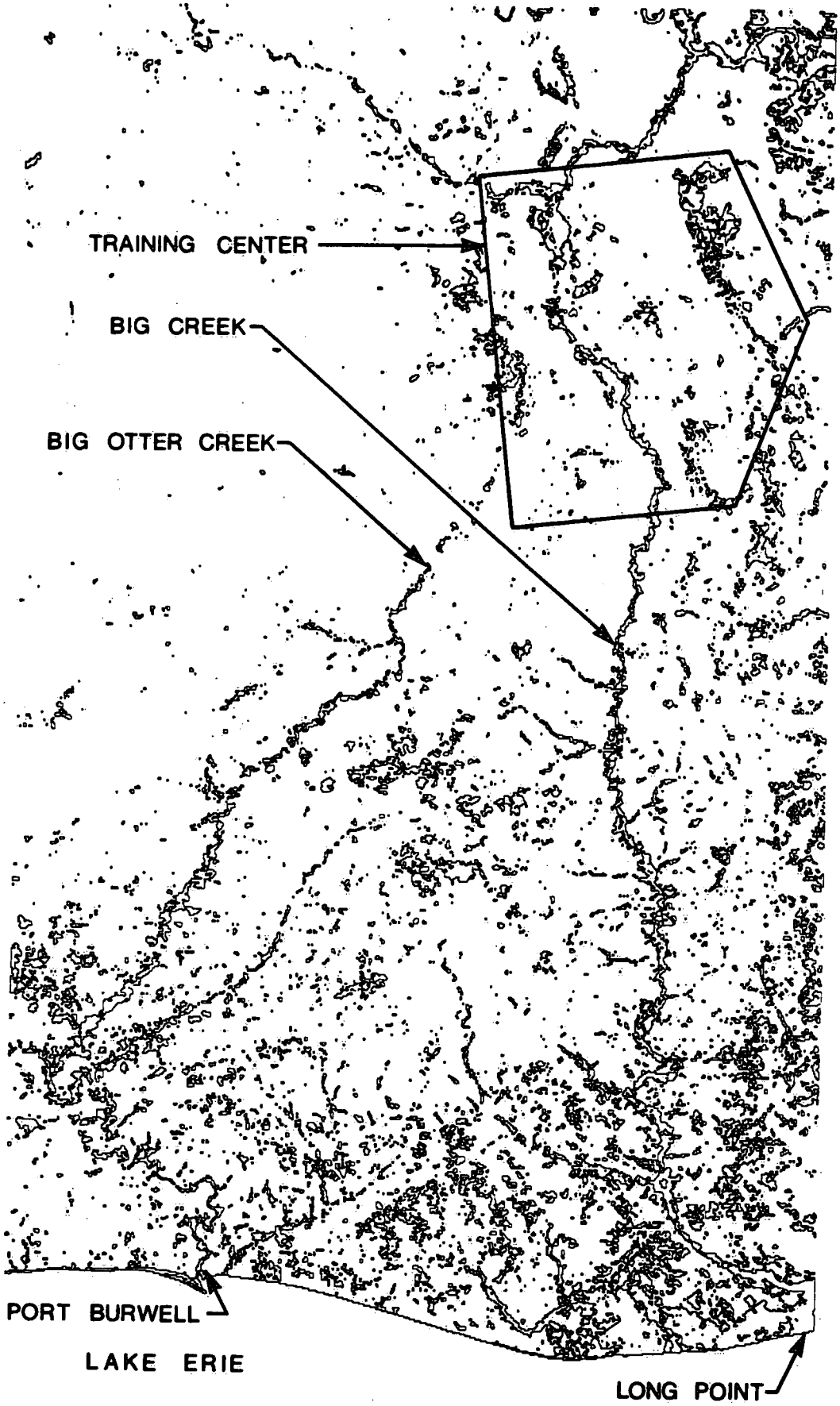
TRAINING CENTER
BIG CREEK
BIG OTTER CREEK
PORT BURWELL
LAKE ERIE
LONG POINT

Figure 11

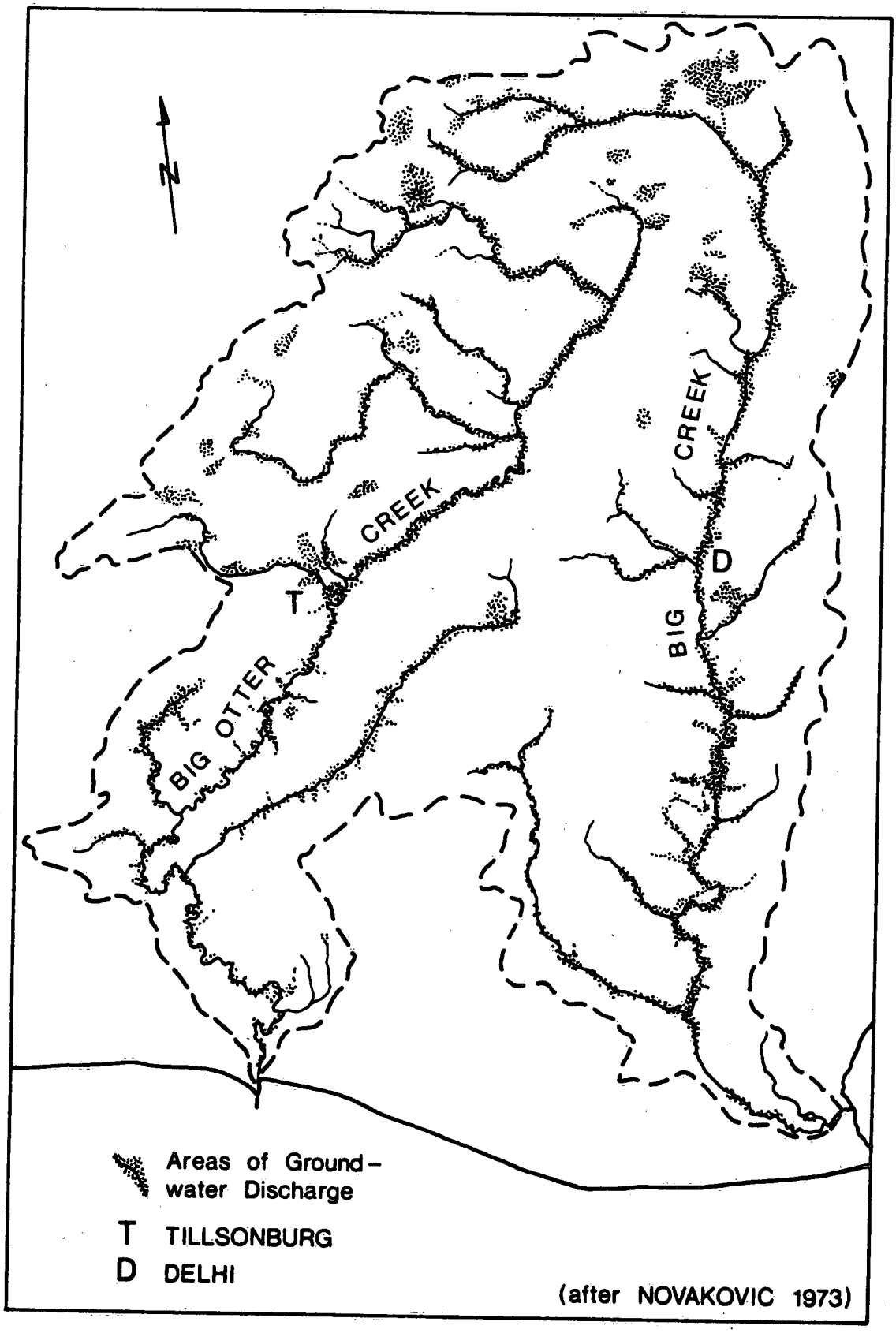

DISTRIBUTION OF GROUNDWATER DISCHARGE AREAS

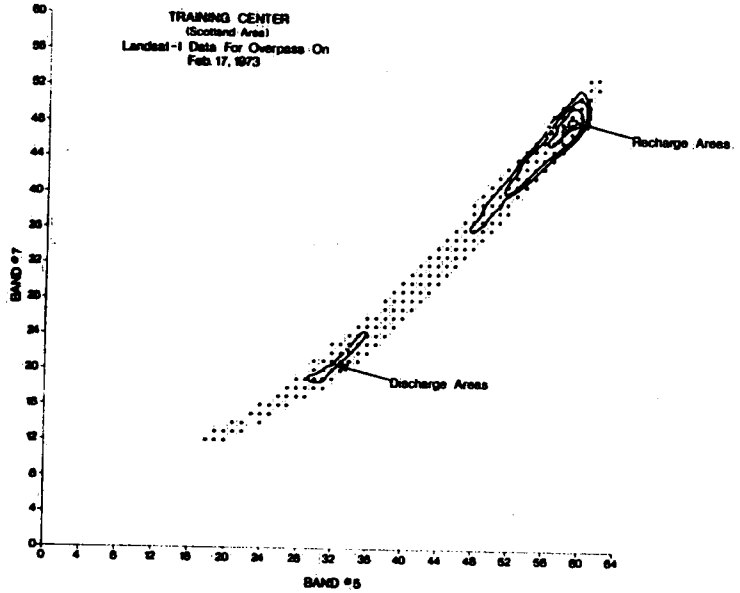
TRAINING CENTER
(Scotland Area)
Landsat-1 Data For Overpass On
Feb. 17, 1973
Recharge Areas
Discharge Areas
BAND # 7
BAND # 5

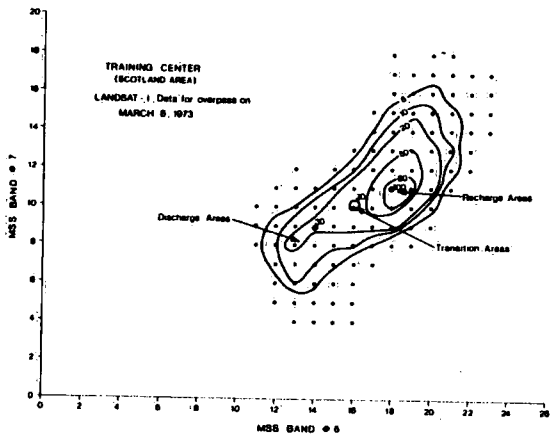
TRAINING CENTER
(SCOTLAND AREA)
LANDSAT - 1 Data for overpass on
MARCH 8, 1973
Discharge Areas
Recharge Areas
Transition Areas
MSS BAND # 7
MSS BAND # 5

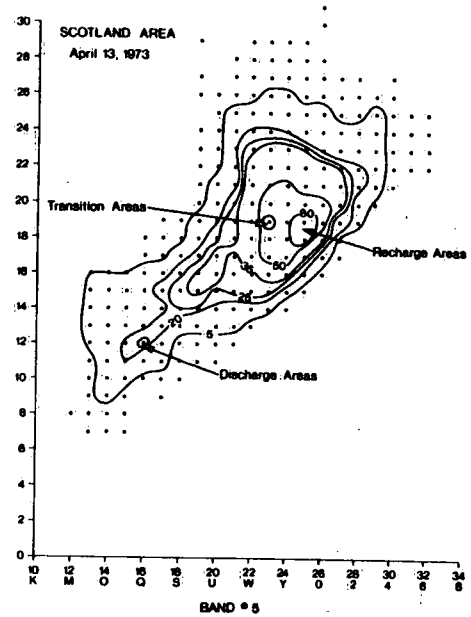
SCOTLAND AREA
April 13, 1973
Transition Areas
Recharge Areas
Discharge Areas
BAND # 5

Figure 12

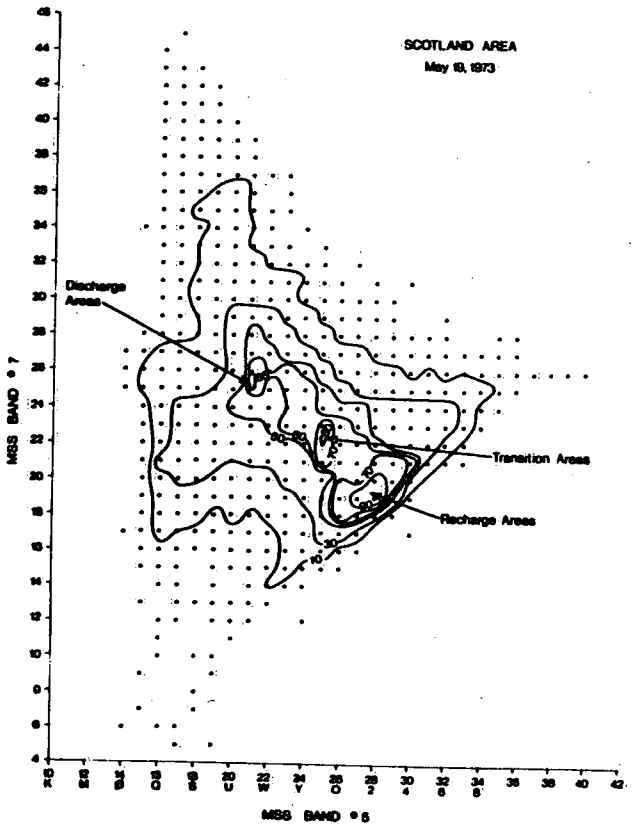
SCOTLAND AREA
May 19, 1973
Discharge Areas
Transition Areas
Recharge Areas
MSS BAND # 7
MSS BAND # 5

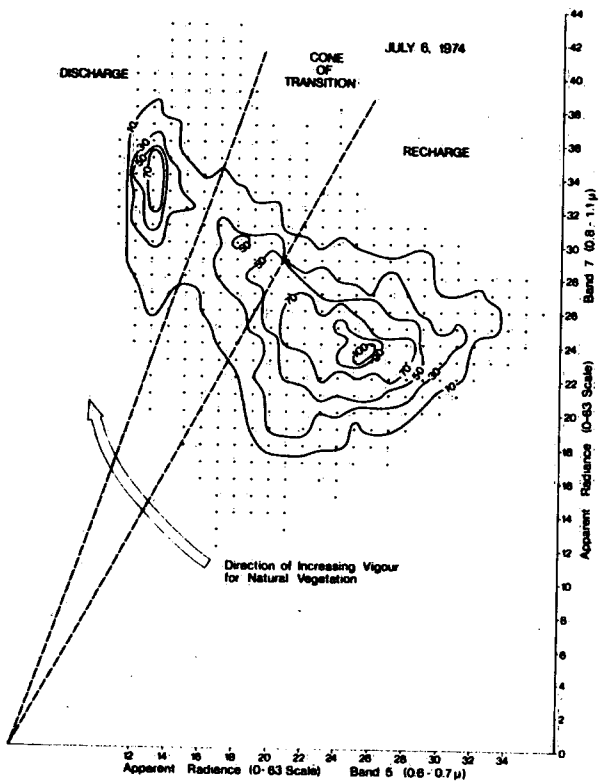
JULY 6, 1974
DISCHARGE
CONE OF TRANSITION
RECHARGE
Direction of Increasing Vigour for Natural Vegetation
Apparent Radience (0-63 Scale) Band 5 (0.6 - 0.7 μ)
Apparent Radience (0-63 Scale) Band 7 (0.8 - 1.1 μ)

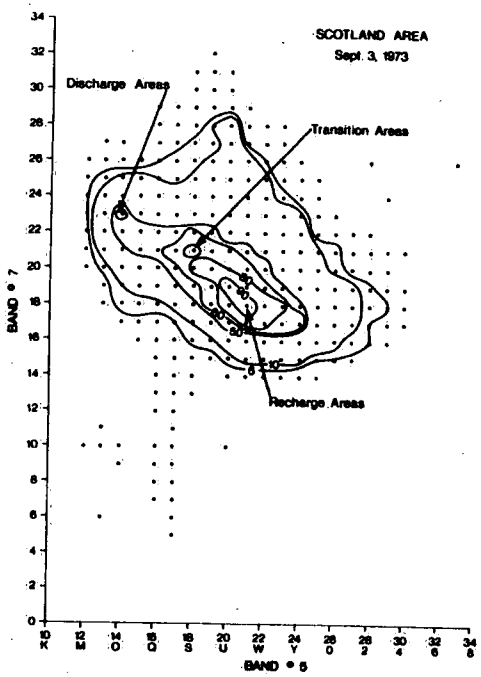
SCOTLAND AREA
Sept. 3, 1973
Discharge Areas
Transition Areas
Recharge Areas
BAND # 7
BAND # 5

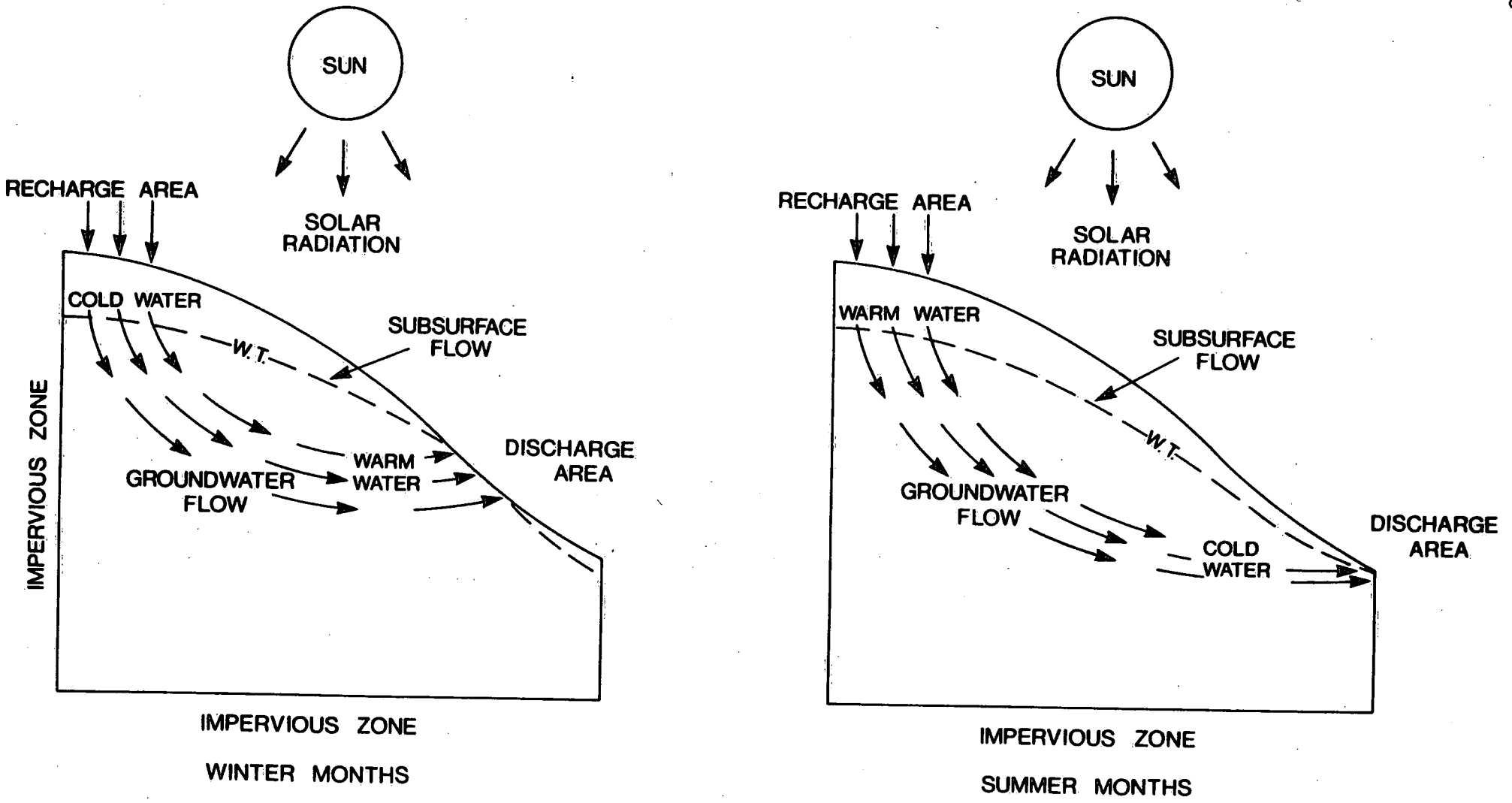
SUN
SOLAR RADIATION
RECHARGE AREA
COLD WATER
W.T.
SUBSURFACE FLOW
IMPERVIOUS ZONE
GROUNDWATER FLOW
WARM WATER
DISCHARGE AREA
IMPERVIOUS ZONE
WINTER MONTHS
SUN
SOLAR RADIATION
RECHARGE AREA
WARM WATER
SUBSURFACE FLOW
W.T.
GROUNDWATER FLOW
COLD WATER
DISCHARGE AREA
IMPERVIOUS ZONE
SUMMER MONTHS

Figure 13